

PAPER • OPEN ACCESS

## Simulation study on the effect of fuel injection and air intake boundary setup on the brake torque response by using comprehensive vehicle model for natural gas vehicle (NGV)

To cite this article: M F A Rahim *et al* 2020 *IOP Conf. Ser.: Mater. Sci. Eng.* **863** 012001

View the [article online](#) for updates and enhancements.

# Simulation study on the effect of fuel injection and air intake boundary setup on the brake torque response by using comprehensive vehicle model for natural gas vehicle (NGV)

M F A Rahim<sup>1,2,\*</sup>, A A Jaafar<sup>2</sup>, Z Taha<sup>2</sup> and R Mamat<sup>3</sup>

<sup>1</sup> Automotive Engineering Research Group, Faculty of Mechanical and Automotive Engineering Technology, Universiti Malaysia Pahang, 26600, Pekan, Pahang, Malaysia.

<sup>2</sup> Innovative Manufacturing, Mechatronics and Sport Laboratory, Faculty of Manufacturing and Mechatronic Engineering Technology, Universiti Malaysia Pahang, 26600, Pekan, Pahang, Malaysia.

<sup>3</sup> Advance Fluid Research Group, Faculty of Mechanical and Automotive Engineering Technology, Universiti Malaysia Pahang, 26600, Pekan, Pahang, Malaysia.

\*E-mail: mfadzil@ump.edu.my

**Abstract.** An analytical, dynamic and comprehensive vehicle model, replicated a high-pressure direct injection compressed natural gas (HPDI-CNG) engine in a vehicle is proposed with the objective to study the effect of fuel injection and air intake boundary condition on the brake torque response. The model simulated the output torque in transient simulations of the natural gas vehicle (NGV) in speed-sweep mode test. The vehicle model has coupled an analytical engine model developed in Simulink with a Simscape driveline model which consists of a clutch model, a simple transmission gear and a simplified vehicle model. In all problem, independent input to the model is the throttle opening ramp. The adjusted parameter in the first study is the methods to calculate the mass of fuel inlet which is based on i) fully experimental data, ii) measured air to fuel ratio (AFR) and (iii) constant injector mass flow rate. In the second problem, the pressure limit of the manifold absolute pressure (MAP) is adjusted as (i) fully experimental data (ii) 1.2 bar (iii) 1.5 bar and (iv) unlimited pressure limit. The dependent parameter in all problem is engine output torque. The results have been compared with the actual data of torque from chassis dynamometer measurement. For the effect of fuel inlet boundary set up, in the fully predictive mode, the model predicted an almost constant maximum torque at a value about 70 Nm, whereas the measured data only produced the same peak value at a very limited instant. If the model used measured AFR as the fuel input boundary, the model overpredicted the maximum peak torque of 70 Nm. In the study on the effect of MAP limit, the maximum torque for 1.2 bar, 1.5 bar and unlimited pressure set up has produced a maximum torque of 45, 62 and 70 Nm, respectively. Results of the first study showed that the use of constant injector mass flow rate has a tendency to simulate an ideal engine acceleration process. The prediction is closed to the measured data if the fuel mass is calculated based on the measured AFR. However, the use of measured AFR in our opinion have reduced the model predictability. In the second study, the increased MAP limit significantly increased the maximum brake torque response. However, the model cannot predict the abnormalities found in the experimental data. The use of MAP limit demonstrated the sensitivity of the output torque on the maximum value of the engine MAP. The results indicated that the injection fuel inlet boundary and the MAP limit have a strong significance on the model prediction and need to be improved for future use of the model.



## 1. Introduction

A new configuration of high-pressure direct injection (HPDI) compressed natural gas (CNG) engine is developed. Gasoline direct injection (GDI) injector was converted to operate with CNG fuel [1]. A model is required to predict the theoretical engine torque as a fundamental performance parameter. Moreover, the use of model-based analysis is a state of art in engineering application nowadays such as in product development and process optimization. Based on previous studies, engine modelling can be categorised based on the modelling technique. There are three general categories which are analytical modelling, the mean-value modelling and finally the system identification modelling [2]. The earliest method is to model the engine processes based on the physical equation for each of the processes. This method is called analytical modelling [3]. The more complex or the more detail process is modelled, the number of equations or the complexities of the equation will increase since each process is considered to produce a realistic prediction [4]. The mean value modelling utilised a simpler approach where certain complex phenomena such as intake flow dynamics or torque generation process are modelled by an empirical equation derived based on experimental data [5]. The generalized empirical model can be coupled with other analytical models for other processes. This model is simpler but the use of the empirical equation required model calibration to be fully generalized for another type of engine. The calibration might be expensive and tedious to perform in practical usage. The system identification engine model is the simplest form of modelling technique for the internal combustion engine. In addition, this type of model has been proven to be the most accurate type of model among others [6], [7]. However, the identification required reliable data for the learning process and lose insight information as the technique required just the input-output data pairs [2]. Hence, an analytical engine model based on thermodynamic single-zone modelling is preferable to analyse detail interaction between parameters. Analytical engine models are mostly consisted the solutions of in-cylinder thermodynamic processes such as progressive combustion, heat transfer, intake and exhaust flow dynamics [8], throttle dynamics [2], and dynamic work transfer from the cylinder piston to the crankshaft [9]. The engine modelled processes may be also coupled with a vehicle model and look-up tables which represent the element of the electronic control unit (ECU) to accurately calculate the engine input parameters. Recently, the model is also expected to be able to simulate the transient condition of engine operation [5,10] to gain a more realistic insight of actual driving condition. Based on the discussed findings, this study is carried out with the purpose to evaluate the effect of fuel injection inlet and air intake boundary condition on the brake torque response by using the new comprehensive model of HPDI-CNG engine. Special case studies have been executed to demonstrate the significance of these critical parameters which affect the prediction accuracies.

## 2. Modelling method

The model developed in the study is proposed to simulate the function of a converted HPDI-CNG prototype vehicle, brand Proton, model Gen.2 which has the specification in table 1. The original gasoline port injection of the engine had been converted to run on CNG by using high-pressure direct injection approach. Since the study was conducted solely based on this vehicle prototype, the proposed model in the current study is developed as similar as possible to the vehicle prototype. The developed analytical engine model in the current study is made of two types of model i) Simulink model ii) Simscape model. Simulink blocks symbolize basic mathematical operations. And linked Simulink blocks are equivalent to a mathematical model or representation of a system under study. Whereas, Simscape blocks dedicated to the modelling of physical components in their actual physical properties.

### 2.1. The simulink model

The Simulink model consisted of the following; the throttle dynamics model to predict the mass flow at the throttle [2], the intake manifold model to predict the manifold absolute pressure which is vital to the ECU [2], and the intake and exhaust valve dynamics which predict the valve curtain flow area [8]. In all section, the one-dimensional compressible flow equation is used and is given by equation (1) [8].

$$\dot{m}_a = \frac{C_d A_{cur} p_o}{(RT)^{0.5}} \left( \frac{p_{st}}{p_o} \right)^{\frac{1}{k}} \left\{ \frac{2k}{k-1} \left[ 1 - \left( \frac{p_{st}}{p_o} \right)^{\frac{k-1}{k}} \right]^{\frac{1}{2}} \right\} \quad (1)$$

The equation (1) is built by the discharge flow coefficient  $C_d$  upstream stagnation pressure,  $p_o$ , static downstream pressure,  $p_{st}$ , the pressure ratio,  $(p_{st}/p_o)$  and the valve curtain area,  $A_{cur}$ .

**Table 1.** Original baseline vehicle and engine specification.

Parameters	Value
<b>Dimension</b>	
Overall length (mm)	4310
Overall width (mm)	1725
Overall height (mm)	1435
Wheelbase (mm)	2600
Tracks (mm)	1475 mm/1470
Weight (kg)	1175 (Auto transmission : 1195)
<b>Engine</b>	
Code	Proton S4PH CAMPRO
Type	In-line 4 cylinders, DOHC, 4 valves per cylinder
Bore/stroke (mm)	76/78
Displacement (cc)	1597
Compression ratio	10:1
Max power (kW)	82 kW @ 6000 rpm
Max. Torque (Nm)	148 Nm @ 4000 rpm
Fuel Delivery	Multipoint EFI
Fuel Cut-Off Point (rpm)	7000 r
ECU	Proton EMS700

The combustion model based on Wiebe method is used to predict the heat release curve [11,12]. The heat transfer model based on Newton heat convection is used to predict the heat loss to the coolant [13] in combination with the empirical model of Hohenberg to calculate the convective heat transfer coefficient [14]. The variation of cylinder volume and cylinder surface area are solved by the solution of kinematics and dynamics of the crank slider mechanism which consider the piston-pin and crankshaft offset [15]. All the sub-models are incorporated within the framework of the modified first law of thermodynamics to solve the in-cylinder pressure and temperature. The cylinder pressure equation is given by equation (2).

$$\frac{dp}{d\theta} = \left( \frac{k-1}{V} \right) \left[ Q_{in} \frac{df}{d\theta} - \frac{hA}{6N} (T_{b,g} - T_w) \right] - \left( k \frac{p}{V} \right) \frac{dV}{d\theta} \quad (2)$$

Major parameters in equation (2) are specific heat ratio,  $k$ , the heat supplied to the cylinder as a function of crank angle,  $Q_{in} \frac{df}{d\theta}$ , the heat loss from the cylinder to the coolant,  $\frac{hA}{6N} (T_{b,g} - T_w)$ , and the cylinder pressure variation due to the boundary work,  $\left( k \frac{p}{V} \right) \frac{dV}{d\theta}$ . The cylinder pressure is then used to determine the dynamic force acting to the piston and transferred to the crankshaft to produce torque pulse. The crankshaft dynamics are modelled in details based on the approach taken by Zweiri et. al [16]. The model considered detail fluctuation of friction components such as piston ring assembly friction torque, the pumping torque, the skirt friction torque. The outcome of the above model is the torque pulse which is then averaged to produce the net mean brake torque and the acceleration of the crankshaft which is used to calculate the engine speed by integration. These outputs are then converted to physical signal and coupled to the SimScape model. The equation for the crankshaft dynamics is given by equation (3).

$$\ddot{\theta}_1 = \frac{1}{\tau \dot{\theta}_1} \left\{ T_{ind} - \left[ M_{pass} r G(\theta_1) G_1(\theta_1) + \frac{1}{2} \frac{\partial J(\theta_1)}{\partial \theta_1} \right] \dot{\theta}_1^2 - \sum_{k=1}^5 T_{fk} - T_S - T_D - T_L \right\} \quad (3)$$

This equation can be coupled to any type of coupling mechanism as founded in the original work of Zweiri et. al [16]. The terms which construct the above equation are the moment of inertia of the engine and crankshaft assembly,  $\tau$ . This value is given by the equation (4).

$$\tau = J_{cran}(\theta_1) + M_{pass} r G(\theta_1) G_2(\theta_1) \quad (4)$$

Other parameters are crankshaft rotational acceleration and rotational speed,  $\ddot{\theta}_1$  and  $\dot{\theta}_2$ , the portion of the reciprocating torque of the engine,  $M_{pass} r G(\theta_1) G_1(\theta_1)$ , the rate of variation of engine inertia due to inner components,  $\frac{\partial J(\theta_1)}{\partial \theta_1}$ , the sum of friction torque due to internal engine assemblies,  $\sum T_{fk}$ , the sum of stiffness torque at the coupling,  $\sum T_S$ , the sum of damping torque at the coupling,  $\sum T_D$ , and The sum of external load implied on the engine,  $\sum T_L$ . The Simulink model inputs are listed in Table 2. The wall surface temperature is assumed to have constant values through-out the engine processes. The total modelled equation in this Simulink model is about 50 equations per each engine cylinder.

**Table 2.** Important input to the Simulink model.

Input parameters	Values
Cylinder wall surface temperature (°C)	420
Bore size (mm)	76
Cylinder stroke (mm)	78
Number of cylinders	4
Compression ratio	10:1
connecting rod length (mm)	132
maximum valve lift (mm)	10
valve diameter (int./ exh.) (mm)	38/32
valve opening angle (int./ exh.) (° BTDC/ °BTDC)	12/ 45
valve closing angle (int./ exh.) (° ABDC/ °ATDC)	48/ 10
engine rotational speed	Feedback from the model output
Instantaneous crank angle	Feedback from the model output

## 2.2. The Simscape model

The SimScape model consists of the clutch model, the simple manual transmission model (considering the test gear only), the final drive model and finally attached to a vehicle model. The input to these models is the acceleration and torque from the crankshaft whereas the model output is the lateral vehicle speed and acceleration as well as the torque at the wheel. The SimScape model directly represents the external load on the engine which needed to be overcome by the engine output. This mimics closely the actual operation of a real vehicle. However, this study will only discuss the engine output torque as the actual focus is on the engine performance parameter. Table 3 presents the inputs to the vehicle model by Simscape.

**Table 3.** Input parameters for the vehicle body used in the simulation.

Parameters	Values
Mass (kg)	1050-1245
Number of the wheel per axle	2
Horizontal distance CG-front axle (m)	1.3
Horizontal distance CG rear axle (m)	1.3
CG height above ground (m)	0.5
Frontal area (m <sup>2</sup> )	3
Drag coefficient	0.4
Initial velocity (mph)	0-20

### 2.3. Multi-cylinder engine synchronization

The actual baseline engine design is a four-cylinder inline engine configuration. Therefore, the formulations of thermo-fluid dynamics presented in Equation (1) to (4) must be accounted for the four cylinders which acting on the same crankshaft. In order to simulate the phasing of the cylinder, the crank angle input to each cylinder must be phased in relative to the crankshaft angle of cylinder 1,  $\theta_1$  following the engine firing order, 1-3-4-2. Hence, the input crankshaft angle for cylinder 3, 4 and 2 is added with the following phase values  $\theta_1 + \pi$ ,  $\theta_1 + 2\pi$  and  $\theta_1 + 3\pi$  respectively.

### 2.4. ECU maps for ignition and injection setup

The developed engine model in the study is governed by the throttle input. The action of the throttle determines the manifold absolute pressure, the amount of air intake, and consequently the cylinder mixture pressure. In addition to that, the throttle action also controlled the amount of fuel injected to the cylinder. This is governed by the use of maps or lookup table which are a common approach in the feedforward control strategy. As in actual ECU of the prototype vehicle, the selection of lookup table values is based on the measured manifold absolute pressure and engine rotational speed. In fact, the table values are similar to the actual table in the actual ECU of the prototype vehicle.

### 2.5. Mean brake torque solution

The actual form of torque transferred from the piston-connecting rod assembly to the crankshaft is in the form of torque pulse. In practical, the damping of the torsional vibration is accomplished by the cylinder balancing procedure. A well-balanced engine cylinder will create a smooth torque transfer which is closed to a mean value of the torque pulse. The balancing calculation is tedious and the computing time will become expensive. Therefore, throughout the study, a cycle-averaging approach has been utilized to obtain the mean brake torque. A variable frequency mean-value quantifier from Simscape toolbox has been used. The instantaneous frequency of the engine is determined from engine speed and used as the quantifier input.

### 2.6. Simulation procedure

The simulation is performed based on speed-sweep test method by providing the ramp input to the throttle pedal of the vehicle. Once throttled, the engine will start to accelerate the vehicle from idle speed to the maximum achievable speed by the engine. As the vehicle speed is changed, all other parameters including the engine input parameters and the output parameters are changes altogether. This test is considered as a transient test as the engine input is changing with time. Two studies have been performed to evaluate the vehicle performances and the setup is presented in table 4 and table 5.

**Table 4.** The simulated cases to study the effect of fuel inlet boundary.

Case	Fuel inlet calculation method	Model's mode
Case 1	Fully measured data	Experiment (baseline data)
Case 2	A measured AFR as the fuel input calculation source and theoretically calculated airflow.	The model with measured input data
Case 3	A constant injector mass flow rate of CNG as the fuel input calculation source and theoretically calculated airflow.	The fully predictive model

**Table 5.** The simulated cases to study the effect of intake air inlet boundary.

Case	Manifold Absolute Pressure (MAP) for Upper Limit
Case 1	1.0 bar (actual ambient pressure)
Case 1	1.2 bar
Case 2	1.5 bar
Case 3	Unlimited

These two cases are crucial since the actual baseline vehicle prototype has been modified to accommodate the CNG direct injection system. The only system which has been added is the fuel injection system for CNG. Furthermore, the ECU has been replaced with a new programmable ECU. The base maps of the ECU have been prepared by professional motorsport tuner in the previous study. Hence, the parameter of the fuel injection system has changed and the performance of the vehicle needs to be reevaluated. Figure 1 presents the layout of the HPDI-CNG engine model.

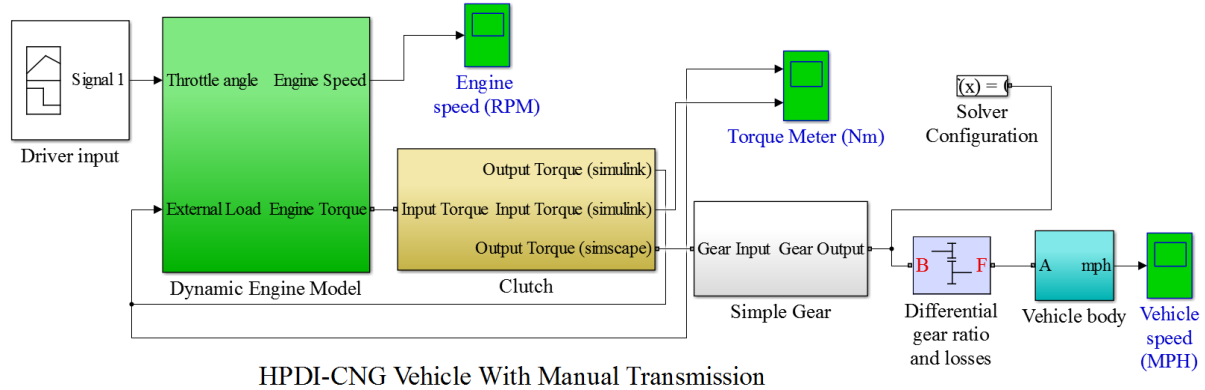


**Figure 1.** Overview of the HPDI-CNG engine model layout.

### 3. Results and discussion

Figure 2 presents the effect of different type of fuel inlet boundary input. Based on the results, the experimental data of Case 1 shown that the torque fluctuated along with the data points. These data points represent the recorded data at an interval of 0.019 seconds where the test was completed in about 18 seconds. From the beginning, it was expected that the fluctuations of the torque were due to the fluctuations of the measured AFR since the AFR affect the combustion pressure and consequently, affect the output torque. Measured AFR from the engine testing produced a randomly fluctuated trends which occurred because of the inefficient driver of the injector. This can be considered as part of the abnormal combustion trend. In order to examine this postulation, the measured AFR data has been imposed as the model input for Case 2. It was proved that the fluctuated, measured AFR data has resulted in a fluctuated engine torque. Even though the model's prediction cannot predict accurately the maximum and minimum value of measured torque, the prediction still able to capture the increment and decrement trends of the brake torque response with a certain amount of delay which is estimated to be about 2.5 seconds in the measured data. The delay between the simulated and measured response exists because the torque response is also dependent on other extraneous parameters such as the engine speed and manifold absolute pressure (MAPS). Different speed and MAP were used by the ECU in the simulations and experiments. In case 3, the response of the brake torque shown an increasing trend at the early of the test time but then produced an almost constant torque until the end of simulation time. When a constant fuel mass flow rate is used as the source for the fuel input boundary calculation, the model produced an almost constant AFR, hence producing an almost constant torque response. When the torque is constant, the speed became constant. And after the speed is feedback into the ECU, it influenced a constant injection duration. Case 3 represents an ideal combustion process of the engine.

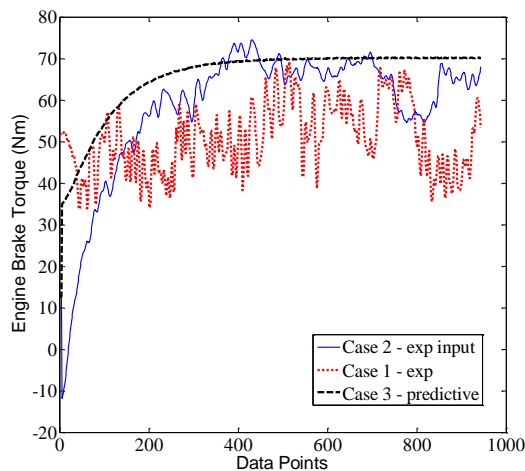


**Figure 2.** Effect of a different method of fuel inlet boundary input on the engine brake torque response in the speed-sweep test procedure.

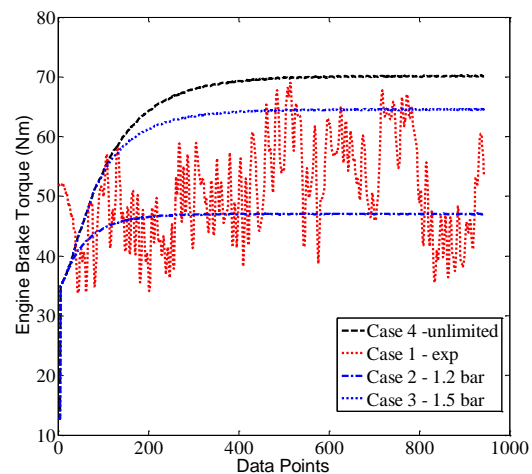


**Figure 3.** Effect of manifold absolute pressure limit on the engine brake torque response in the speed-sweep test procedure.

Figure 3 presents the plot of manifold absolute pressure limit effect on the engine brake torque response for the speed-sweep test procedure. For all simulated cases, the results trend shown a brake torque response which increased from zero at the start of the simulation until the peak torque is achieved and then constant until the end of the simulated time. Basically, the model took a minor time to adjust the initial torque response based on the model's initial conditions and then the torque prediction sharply increased to a value of about 35 Nm. The simulations are performed based on the full predictive model with a constant mass flow rate of fuel. The discussion of figure 2 has explained how the torque has become constant along the simulated time. Again, the model predicted ideal cases hence it cannot predict the abnormal combustion phenomena existed in the experimental result. Results in figure 3 also demonstrate that the engine torque response is highly affected by the MAP limit setting in the model. As the MAP limit is increased, the maximum engine brake torque response increased significantly. The maximum brake torque response is predicted when the MAP limit is set as unlimited at a value of 70 Nm. This is easily understood since the limit of MAP allows the use of greater manifold pressure to calculate the intake of fresh air. The higher the intake manifold pressure, then the easier for the engine to induce fresh air into the cylinder. When the amount of fresh air is increased, more fuel is allowed to be oxidized and produced greater heat release to be transformed as useful brake torque. As the MAP is restricted to 1.5 bar and 1.2 bar, the maximum torque produced is limited to a value of about 62 Nm and 45 Nm respectively. In actual condition, the MAP sensor only detected the manifold pressure value up to 1.04 bar only. The maximum value is slightly higher than the ambient pressure of 1.01 bar. This is true for normal aspirated (NA) internal combustion engine. The simulated cases aren't out of practice but have demonstrated how sensitive the output torque to the MAP limit setup. Review on the other MAP calculation parameters such as the estimated manifold volume and intake air temperature is suggested to further improve the calculation accuracy.

#### 4. Conclusion

The comprehensive model developed in the study unable to predict the abnormal combustion existed in the actual engine. The model predicted the ideal combustion process through the use of a fully predictive setting. However, if the model is provided with actual input data from the experiment, the prediction is improved in which the results are getting closer to the measured engine torque trends. For the effect of fuel inlet boundary set up, in the fully predictive mode, the model predicted an almost constant maximum torque at a value about 70 Nm, whereas the measured data only produced the same peak value at a very limited instant. If the model used measured AFR as the fuel input boundary, the model overpredicted

the maximum peak pressure of 70 bar. In the study on the effect of MAP limit, the maximum torque for 1.2 bar, 1.5 bar and unlimited pressure set up has produced a maximum torque of 45 bar, 62 bar and 70 bar respectively. The simulated case studies for both problems proved that the fuel boundary setup and the limit of manifold absolute pressure in the intake air calculation are vital since the changes in the boundary types and values affected the results significantly in term of magnitudes and trends. However, the use of measured AFR as the input to calculate the amount of fuel supplied to the cylinder has reduced the predictability of the model. And a suitable limit of MAP is needed for future use of the model. Finally, the model needed to be improved in both aspects of set up to improve the simulation accuracy.

### Acknowledgements

We would like to express our sincere gratitude to The Ministry of Education and Universiti Malaysia Pahang who has funded the study under research grant numbered FRGS/1/2017/TK03/UMP/03/2 and RDU1703145, members of Automotive Laboratory, and Innovative Manufacturing, Mechatronics and Sports laboratory which facilitate the study from the beginning.

### References

- [1] Z. Taha, M. Abdul Rahim, and R. Mamat, "Injection characteristics study of high-pressure direct injector for compressed natural gas ( CNG ) using an experimental and analytical method."
- [2] A. Pezouvanis, "ENGINE MODELLING FOR VIRTUAL MAPPING," University of Bradford, 2010.
- [3] S. R. Krishnan and K. K. Srinivasan, "Proceedings of the Institution of Mechanical Engineers, Part D : Journal of Automobile Engineering," 2010.
- [4] A. Chow and M. L. Wyszynski, "Thermodynamic modelling of complete engine systems - a review," *Proc. Inst. Mech. Eng. Part D-Journal Automob. Eng.*, vol. 213, no. D4, pp. 403–415, 1999.
- [5] M. Grahn, J. O. Olsson, and T. McKelvey, "A diesel engine model for dynamic drive cycle simulations," *IFAC Proc. Vol.*, vol. 18, no. PART 1, pp. 11833–11838, 2011.
- [6] S. J. Rutherford and D. J. Cole, "Modelling nonlinear vehicle dynamics with neural networks," *Int. J. Veh. Des.*, vol. 53, no. 4, pp. 260–287, 2010.
- [7] K. Shimojo, Y. Kitamura, M. Sato, M. S. Vogels, M. Reumueller, and L. Lackner, "Global dynamic modelling for gasoline engine," *IFAC Proc. Vol.*, vol. 7, no. PART 1, pp. 695–699, 2013.
- [8] S. Sitthiracha, "An analytical model of spark ignition engine for performance prediction," in *The 20th Conference of Mechanical Engineering Network of Thailand*, 2006, no. October, pp. 1–60.
- [9] Y. H. Zweiri, J. F. Whidborne, and L. D. Seneviratne, "Complete Analytical Model of a Single-Cylinder Diesel Engine for Non-linear Control and Estimation," 1999.
- [10] M. Grahn and M. Grahn, *Model-Based Diesel Engine Management System Optimization A Strategy for Transient Engine Operation*. 2013.
- [11] S. Rousseau, B. Lemoult, and M. Tazerout, "Combustion characterization of natural gas in a lean-burn spark-ignition engine," *Proc. Inst. Mech. Eng. Part D J. Automob. Eng.*, vol. 213, no. 5, pp. 481–489, Jan. 1999.
- [12] J. I. Ghojel, "Review of the development and applications of the Wiebe function: A tribute to the contribution of Ivan Wiebe to engine research," *Int. J. Engine Res.*, vol. 11, no. 4, pp. 297–312, 2010.
- [13] E. Neshat and R. K. Saray, "Effect of different heat transfer models on HCCI engine simulation," *Energy Convers. Manag.*, vol. 88, pp. 1–14, 2014.
- [14] H. S. Soyhan, H. Yasar, H. Walmsley, B. Head, G. T. Kalghatgi, and C. Sorousbay, "Evaluation of heat transfer correlations for HCCI engine modelling," *Appl. Therm. Eng.*, vol. 29, no. 2–3, pp. 541–549, 2009.

- [15] K. Tripathi and H. Ranjangaonkar, “Kinematic and Dynamic Modeling and Simulation of Four Stroke Petrol Engine,” *Int. J. Eng. Res. Appl.*, vol. 4, no. 6, pp. 54–57, 2014.
- [16] Y. H. Zweiri, J. F. Whidborne, and L. D. Seneviratne, “Detailed analytical model of a single-cylinder Diesel engine in the crank-angle domain,” *Proc. IMechE, Part D J. Automob. Eng.*, vol. 215, no. 11, pp. 1197–1216, 2001.